

## Structural effects of element substitution on superconducting properties in 1-2-3 YBCO : an electron microscopy study

G. Van Tendeloo, T. Krekels, O. Milat, S. Amelinckx

University of Antwerp (RUCA),  
Groenenborgerlaan 171, B 2020 Antwerpen, Belgium

### Abstract

Changes in the crystal structure or the microstructure, as a result of different substitutions in  $\text{YBa}_2\text{Cu}_3\text{O}_7$  have been studied by electron microscopy and have been related to the physical properties of these substituted materials. Oxygen ordering has been investigated in superconducting  $\text{ABa}_2\text{Cu}_3\text{O}_{7-\delta}$  ceramic materials with  $A=\text{Er, Nd, Sm, Y}$  and  $\text{Yb}$ , as well as in samples of this type with the rare earth  $A$  partially substituted by  $\text{Pr}$ . The critical temperature  $T_c$  was determined as a function of the oxygen deficiency of the compound. A distinct relationship exists between the width of the 60K plateau and the OrthoII ordering. Our results show that the OrthoII ordered phase is the superconducting phase with a characteristic  $T_c$  of 60K. Small Fe substitutions for Cu have a dramatic impact on  $T_c$  as well as on the microstructure. The twin domain size decreases and a "tweed" pattern results. Randomly dispersed Fe-ions or Fe-clusters act as pinning centers for twin interfaces. Substituting Ga or Co for Cu changes the structure of the "chain" layer. A model for a new superstructure ordering in this chain layer of Ga and Co substituted 1-2-3 YBCO is proposed.

### 1. Introduction

$\text{YBa}_2\text{Cu}_3\text{O}_{7-\delta}$  is by far the most widely studied ceramic superconductor. Its (perfect) structure for  $\delta = 0$  is long known and the effect of oxygen deficiency has been extensively studied (SEE e.g. [1,2]). Excellent thin films have been produced (e.g. [3,4]) and the effects of processing on the superconducting properties have been extensively studied.

Doping of such superconducting materials by isomorphous substitution of aliovalent ions and studying the effect of doping on the superconducting properties has proved to be a successful method to gain information on the structural requirements for the occurrence of superconductivity and it allows to optimize its properties [5].  $\text{YBa}_2\text{Cu}_3\text{O}_7$  is extremely tolerant in accepting various substitutions without profoundly modifying its structural features, even though the superconducting properties may be severely altered [6]. An important conclusion of all these experiments is that the structural integrity of the  $\text{CuO}_2$  layer seems to be essential for the occurrence of superconductivity [7]. The stoichiometry and the dopant atoms in the  $\text{CuO}$ -layer are important in determining the number and the type of charge carriers [8].

In this paper we will try to present an overview of structural studies of different YBCO rela-

ted materials. Most materials treated here are obtained by substitution of one of the YBCO components. We will consider the substitution of Y by other rare earth elements and at the same time oxygen for vacancies [9]; Cu by Fe, Al, Zn, Au etc.[10,11]; Ba by Sr, however this is not successful unless one simultaneously substitutes Cu by e.g. Co or Ga [12,13].

Structural characterisation is performed by electron diffraction and electron microscopy at the "Electron Microscopy for Materials Research" center of the University of Antwerp.

An almost trivial substitution is that of oxygen by vacancies in the composition range  $1 \geq \delta \geq 0$ . Apart from the formation of a  $\sqrt{2}a \times \sqrt{2}a$  superstructure (close to a composition  $\delta=1$ ) attributed to a 2D modulation in the  $\text{CuO}_2$  layer [14], all oxygen substitutions only affect the  $\text{CuO}$  layer configuration. As a function of the oxygen deficiency different orthorhombic superstructures, termed Ortho II, Ortho III, etc. have been reported [15,16], most of them first discovered by electron diffraction. For some time a discussion has been going on concerning the correlation between these superstructures and the behaviour of  $T_c$  as function of oxygen content. Is the so called Ortho II structure responsible for the 60 K plateau in the  $T_c$ /oxygen content curve? We will provide some more arguments with respect to this problem by substituting Y by rare earth ions of different size.

## 2. Substitution of Y by Er, Nd, Pr, Sm or Yb.

In the fully oxidated state  $O_{7-\delta}$  (with  $\delta=0$ ), the basic orthorhombic structure (Ortho I) is formed for the Y compound as well as for all substituted compounds. CuO chains are formed along the **b**-axis by ordering of oxygen atoms into sites along **b** in between every two Cu atoms of the square Cu lattice. In the Ortho II phase, which has an ideal oxygen content of 6.5, the oxygen atoms of every other copper-oxygen chain are missing; the unit cell doubles along the **a**-axis and therefore this superstructure is sometimes also called the  $2a_0$  structure. The appearance of this superstructure is often related to the presence of a plateau at about 60K in the  $T_c$  versus oxygen content curve of well annealed samples.[15,16] In the case of

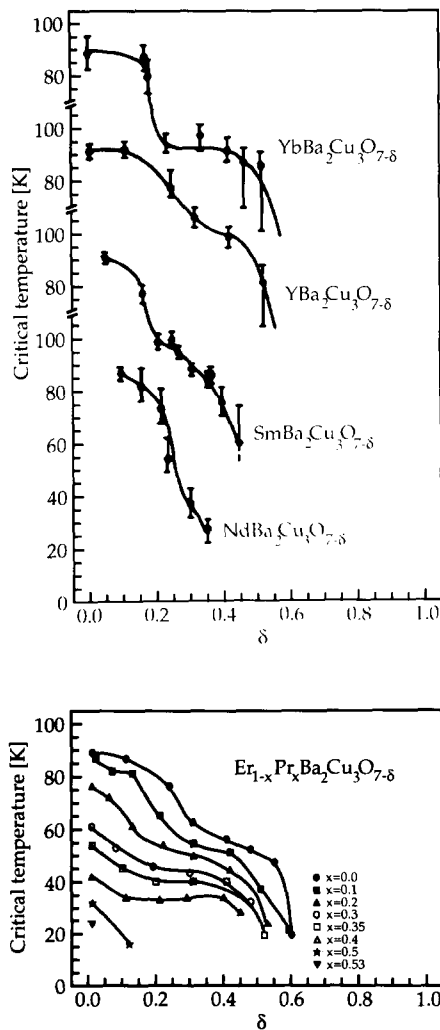


Fig. 1. (a)  $T_c$  versus oxygen concentration  $\delta$  for  $ABa_2Cu_3O_{7-\delta}$  with  $A = Yb, Y, Sm$  and  $Nd$  respectively.. (b) Same graph for  $Er_{1-x}Pr_xBa_2Cu_3O_{7-\delta}$ .

quenched samples no plateau is observed and the critical temperature decreases monotonically with increasing oxygen deficiency.[17] In such material, no or very ill defined Ortho II superstructures are detected.[16]

Recently, Buchgeister et al. replaced in a systematic way the Y ion by different rare earth ions and established a close relationship between the ion size of the substituted rare earth and the different structural and electrical properties of the material [18,19]. Apart from a weak dependence of orthorhombicity on the ionic radius of the rare earth ion, a variation was observed of the width of the 60 K plateau. A pronounced plateau appeared for the smaller ions (Yb, Er, Y) while for the larger ions (Nd,La) no plateau was observed at all (fig.1a).

Electron diffraction of these materials was carried out at 100 kV [9]. For the smaller ions, very clear and well defined extra Ortho II or  $2a_0$  ordering reflections were detected in the [001] zone pattern (fig.2a). Best defined ordering occurred (for all compounds studied) at oxygen contents around  $O_{6.6}$ . Dark field imaging in these sharp reflections reveals the  $2a_0$  ordered domains as bright specks (fig.3a); the domains are fairly isotropic and the size exceeds several tens of nm. Usually the extra diffraction spots are elongated along  $a^*$ , particularly for oxygen

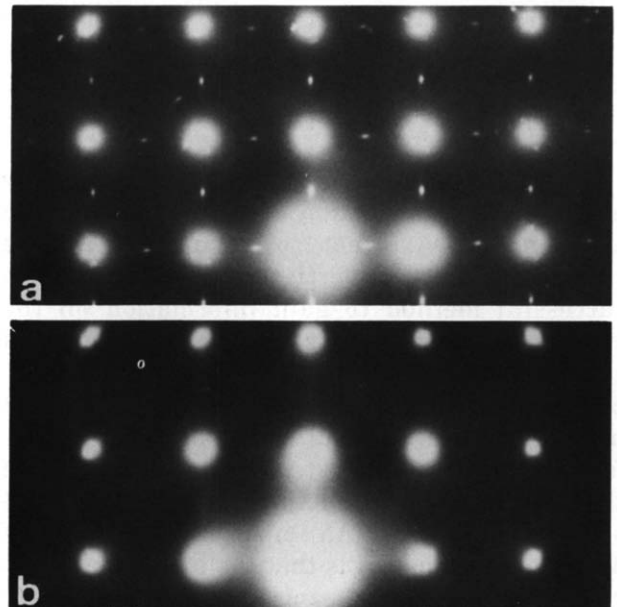


Fig. 2 [001] diffraction patterns from different  $ABa_2Cu_3O_{7-\delta}$  materials. (a) Sharp superlattice reflections are present in well ordered Ortho II material for  $A = Yb$  or  $Y$ . (b) Only very ill defined [100]\* streaking is observed when  $A = Nd$ .

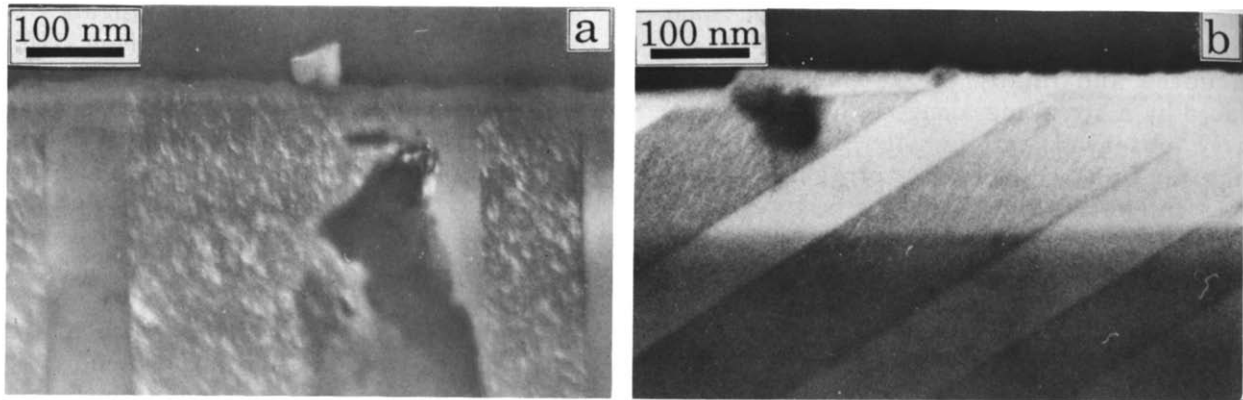


Fig. 3 Dark field image showing Ortho II ordered domains as bright speckles.

concentrations corresponding to the edges of the 60K plateau. The corresponding  $2a_0$  domain sizes are now lenticular in shape and their size decreases with the distance from the middle of the plateau (fig 3b). For the larger ions (e.g. Nd) the corresponding [001] pattern only showed a weak diffuse scattering along the  $[100]^*$  and  $[010]^*$  directions (fig.2b). Attempts to image the domains corresponding to such weak diffuse intensity failed in all cases.

In these measurements a clear correlation between the presence of the Ortho II structure and the presence of a 60 K plateau is established. This correspondence is further supported by experiments performed on Pr-doped samples. With increasing Pr-content the critical temperature of the higher  $T_c$  plateau (93 K) is suppressed relative to the lower  $T_c$  plateau to a level where the  $T_c$ 's of both plateaus meet (fig.1b).[18,19] The  $T_c$  of the lower plateau is only slightly affected by the doping and also the Ortho II superstructure is not affected.

We conclude that an unambiguous correlation exists between the superconducting 60 K phase and the structural Ortho II phase.

## 2. (Limited) substitution of Cu by Fe, Zn, Au, ...

Limited amounts of Cu (up to 5%) were substituted by different metals such as Fe, Al, Zn, Au, ... For all substitutions, except for Au additions, the critical temperature decreases drastically upon adding foreign elements (see e.g. [20,21]). Together with this decrease in  $T_c$  we notice definite changes in the microstructural configuration. We will elaborate somewhat on

the Fe substitution, but more details such as specimen preparation can be found in [10,11].

Undoped 1-2-3 YBCO material normally exhibits wide and more or less regularly spaced (110) and  $(\bar{1}\bar{1}0)$  twin bands; the separation between subsequent interfaces is approximately 100 nm. [001] type diffraction patterns over such twin interfaces exhibit a characteristic spot splitting, which allows to deduce the orthorhombicity and indirectly also the (local) oxygen content. Such a pattern from a fully

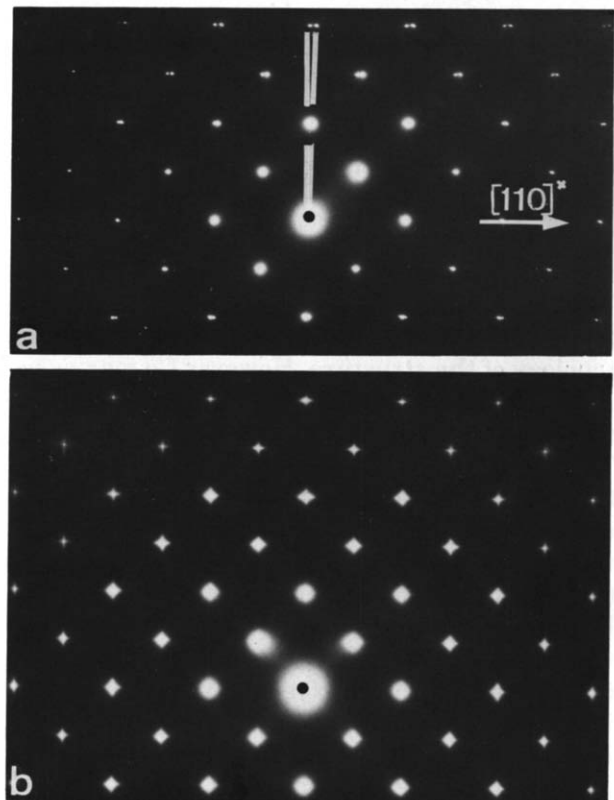


Fig.4 [001] electron diffraction patterns of undoped (a) and Fe-doped 1-2-3 YBCO (b).

oxidized sample is reproduced in fig. 4a. Upon Fe-doping the spot splitting becomes less pronounced and finally the two satellites are replaced by a streaking along  $[110]^*$  and  $[\bar{1}\bar{1}0]^*$ , clearly observed in fig. 4b. The average structure finally becomes tetragonal. This diffraction effect is the result of a fragmentation in real space of the structure in micro-twin domains. For limited substitutions, iron ions have been shown to substitute Cu(1) atoms in the CuO chain layer [22] where they pin the interfaces, in agreement with a decreasing twin size for increasing iron content.[10] For the more strongly doped materials, individual twin interfaces can no longer be discerned and a tweed structure develops. Although the average structure is tetragonal, locally orthorhombic distortions are still present; This can be concluded from high resolution images of a such tweed structure. Optical diffraction (fourier transforms) of limited areas of the high resolution image reveal the orthorhombic distortion. At high iron content and with the right heat treatment, the twin bands persist but a fine tweed structure is superimposed. The reason of this fine tweed structure has been associated with the presence of strain fields caused by iron ions or iron clusters not located along the (110) type interfaces.[10]

### 3. Substitution of Ba by Sr and Cu by Co or Ga.

The isostructural compounds  $\text{YSr}_2\text{Cu}_2\text{CoO}_7$  and  $\text{YSr}_2\text{Cu}_2\text{GaO}_7$  are closely related to the 1-2-3 YBCO compound. Replacement of Ba by Sr (or by a mixture of Sr and Ce) does not change the topology of the structure. However Co ions as well as Ga ions have a strong tendency to be tetrahedrally coordinated by oxygen ions.[12,13] Therefore the CoO or GaO layers, which replace the CuO chain layer, adopt a configuration of chains of corner sharing  $\text{MO}_4$  ( $M = \text{Co}, \text{Ga}$ ) tetrahedra along the  $[110]_p$  and  $[\bar{1}\bar{1}0]_p$  directions (index p refers to the perovskite base). The CuO-layer configuration of the YBCO compound is compared to the MO-layer configuration in fig. 5. The tetrahedron of oxygen atoms around the M ion consists of the two oxygen atoms of the SrO-layer forming the apices of the  $\text{CuO}_5$  pyramid and of two oxygen atoms in the MO-layer. In reality these tetrahedra are rotated about an axis parallel to c. This rotation can take place in two

"a priori" equally probable senses, giving rise to zig-zag chains of opposite "phase" along  $[110]_p$  or  $[\bar{1}\bar{1}0]_p$  (see fig.5b). We can call such parallel chains left (L) and right (R). In the structure described by Roth et al. [12] all chains are either all L-chains or all R-chains. Note that R- and L-chains have identical surroundings and hence are energetically equivalent.

The basic unit cell (with all chains parallel and of the same type) is described by a rectangular quasi-square mesh with  $a_0 \approx b_0 = \sqrt{2}a_p$ , where  $a_0$  is chosen perpendicular to the chains. In the compounds studied the chains are parallel in two MO-layers successive along  $c_0$  and are shifted with respect to each other in such a way that they form a staggered arrangement when they are viewed end-on.

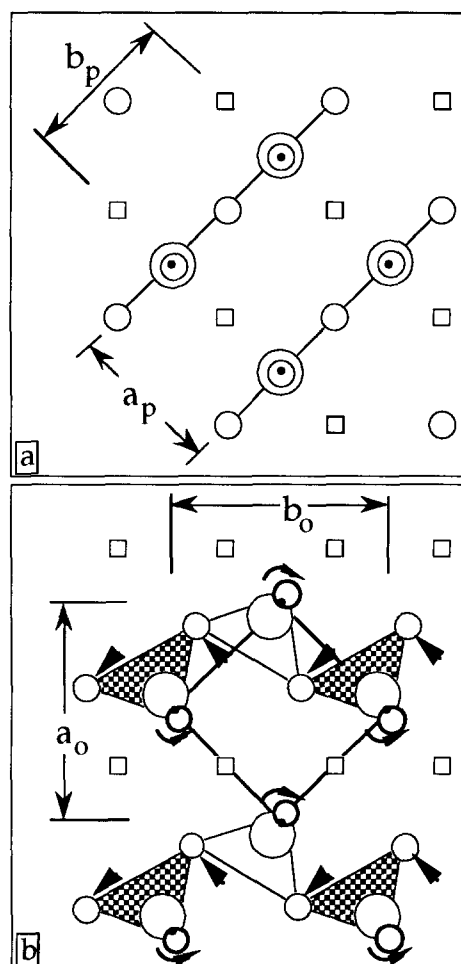


Fig. 5 Schematic representation of the atom configuration of (a) the CuO chain layer in  $\text{YBa}_2\text{Cu}_3\text{O}_7$ , with a square configuration of O around Cu and (b) the MO layer, showing the chains of tetrahedra along the  $[110]_p$  direction. Large circles are M-ions, small circles are oxygen ions. Vacancies are indicated by squares.

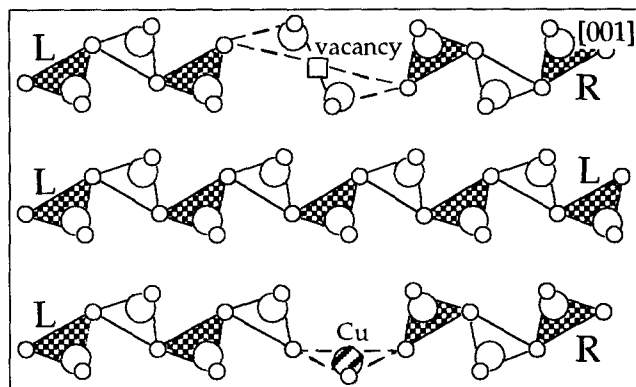


Fig. 6 Schematic representation of MO chains. The presence of a vacancy or a copper ion may induce an L-chain to become an R-chain and vice versa.

We will present evidence that within a single layer a superstructure  $2a_0 \times b_0$  is formed due to a regular alternation of L- and R-chains along the  $a_0$  axis. Such an ordered arrangement of tetrahedra may exhibit different types of disorder :

a) an L-chain may change into an R-chain; this is possible when a vacancy is introduced or when an occasional planarly coordinated copper ion replaces the M-ion. (see fig. 6)

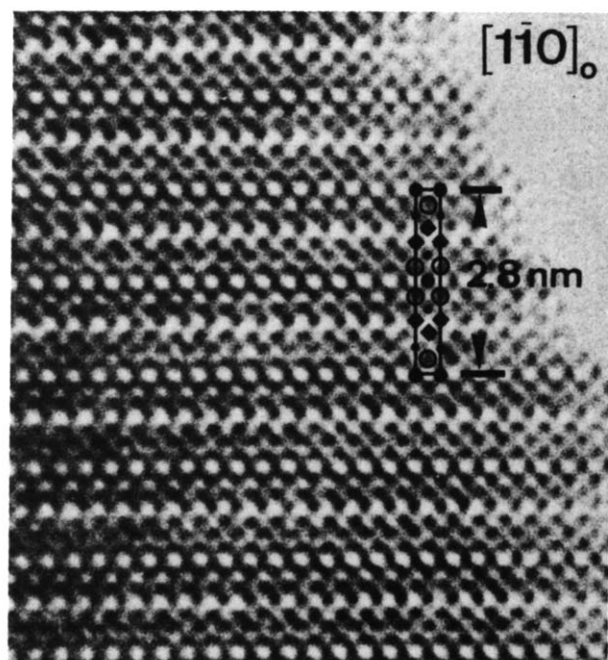


Fig. 7 High resolution image of the Ga-2212-compound along the  $[1\bar{1}0]_0$  zone. The atom columns are imaged as dark dots. The open dots represent strontium columns, the squares represent the rare-earth columns in the fluorite-like lamella. The large full dots represent Ga atom columns, the small full dots represent copper atoms in the  $\text{CuO}_2$  layers. Oxygen atoms are not imaged.

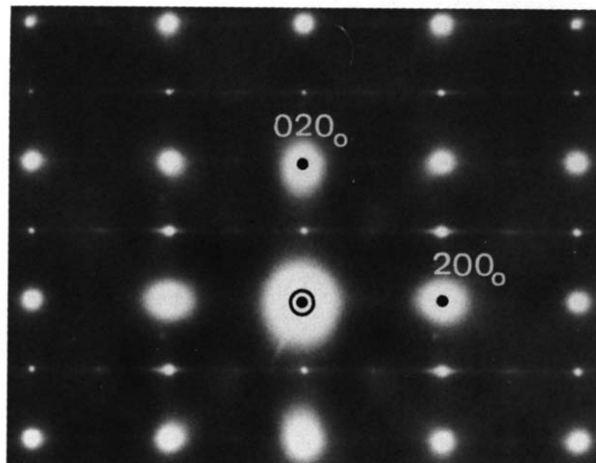


Fig. 8  $[001]$  diffraction pattern for the Ga-1212.

b) within a single layer the L-R-alternation of chains shows deviations (e. g. LRRLR).

c) within a single layer at a twin line the chain arrangement may change its orientation by  $90^\circ$  (from  $[110]_p$  to  $[\bar{1}\bar{1}0]_p$  due to the presence of Cu ions in the MO layer).

d) in between successive MO-layers along the  $c$ -direction stacking disorder may exist. Several of these defects have been observed by high resolution electron microscopy.[23,24] Some examples will be presented below.

The Y-layer, which in the basic 1-2-3 YBCO compound is oxygen free, can be replaced by a fluorite-like lamella of  $(\text{Nd,Ce})\text{O}_2$  in the  $(\text{Nd,Ce})_n\text{O}_{2n}\text{Sr}_2\text{GaCu}_2\text{O}_5$  compounds. These compounds form a homologous series of mixed layer compounds with  $n = 1, 2, 3, \dots$  [25,26]; they can be easily distinguished by their  $c$ -parameter, which obviously increases with  $n$ . In the high resolution image of fig. 7 the  $n = 2$  compound viewed along the perovskite  $[100]$  direction is shown. The different layers in the sequence ... - GaO - SrO -  $\text{CuO}_2$  -  $(\text{Nd/Ce})\text{O}_2(\text{Nd/Ce})$  -  $\text{CuO}_2$  - SrO - ... can be identified from symmetry considerations or by image simulations.

Superconductivity was recently reported with a  $T_c$  up to 50K in the Ca doped Ga-substituted compounds  $\text{Ln}_{1-x}\text{Ca}_x\text{Sr}_2\text{GaCu}_2\text{O}_7$  [27].

Electron diffraction observations along a number of simple crystallographic zones show apart from the basic reflections extra satellites and diffuse scattering, indicating that several aspects of the disorder mentioned above are indeed occurring in reality. In fig. 8 for instance, the  $[001]$  zone is shown for the Co-substituted compound. The intense reflections

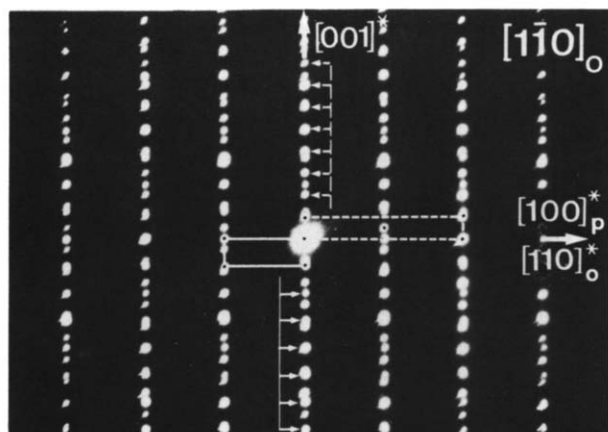


Fig. 9 Diffraction pattern of the n212-Ga intergrowth structure along the  $[110]_O$  zone. The selected area contains two phases with different  $c$ -parameters:  $c^{(1)} = 2.28$  nm;  $c^{(2)} = 2.82$  nm, corresponding with compounds containing respectively a single and a double fluorite-like lamella.

are due to the perovskite structure, while the weak spots are due to a superstructure with parameters  $2a_0, b_0, c_0$ . Different sections allow to reconstruct the reciprocal space, as well for the Co-substituted 1212 compound as for the Ga-substituted n212 compound.

Often, intergrowth structures (corresponding to different  $n$ -values) of this latter compound occur; they are easily identified on electron

diffraction patterns. Note that the two superimposed patterns have different geometrical features. The pattern corresponding to the smaller  $c$ -spacing ( $c_1 = 2.28$  nm) has a rectangular mesh (outlined by solid lines) showing that the orthorhombic reciprocal cell is not body centered; this is consistent with the presence of a single rare earth layer in the structure. The pattern corresponding to the larger  $c$ -spacing ( $c_2 = 2.82$  nm) has a centered unit mesh outlined by dotted lines; it shows that this reciprocal unit cell is body centered, which is consistent with the presence of a double layer rare earth oxide lamella, causing a relative shift between successive perovskite blocks.

High resolution images such as the  $[010]_O$  or  $[100]_O$  image of fig.10 illustrate the presence of several defects. The left part shows a  $[100]_O$  image while in the right part image a  $[010]_O$  type image is observed. This indicates a  $90^\circ$  change in the orientation of the the chains. Along the  $[010]_O$  direction the the CoO-chains are imaged as rows of dots separated by 0.54 nm; the image proves that along this direction the chains occur in a staggered arrangement.

The superstructure, introduced by a regular alternation of L- and R-chains within a CoO or GaO layer can clearly be observed in sections

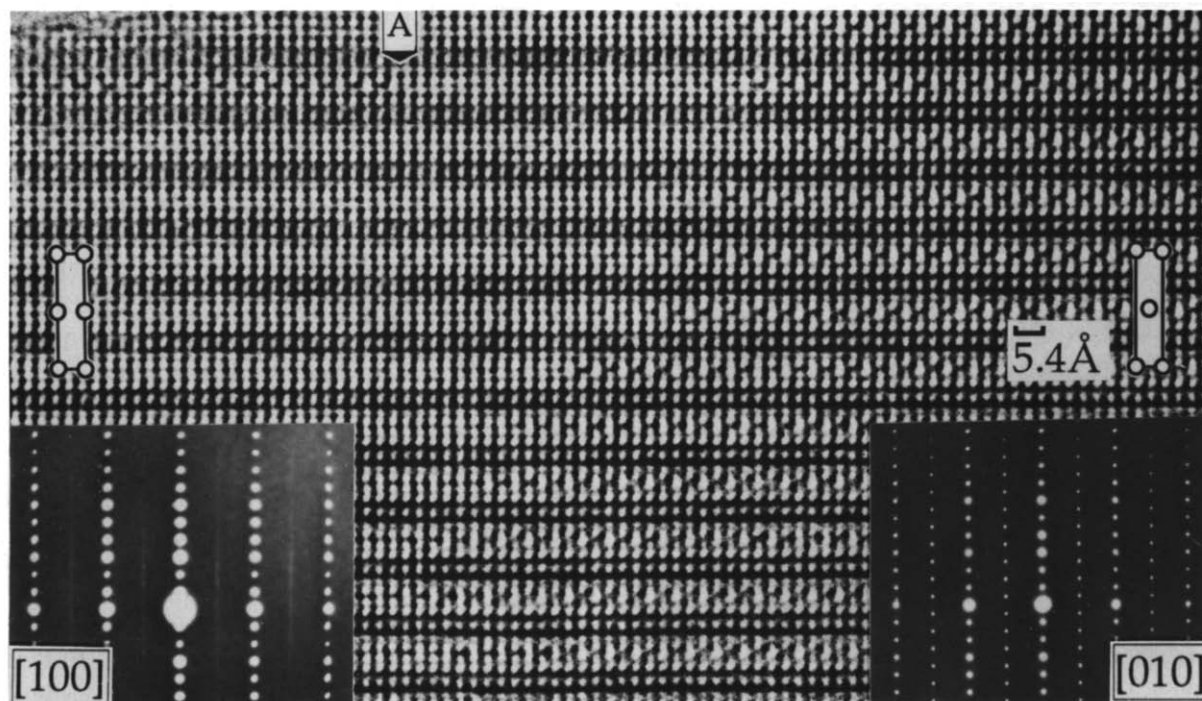


Fig. 10 High resolution image of the Co-1212 phase containing two orientation variants of the superstructure. In the left part the image is viewed along the  $[001]_S$ , in the right part the chains are viewed along their length axis. The arrangement in the Co-layer is indicated in both parts.

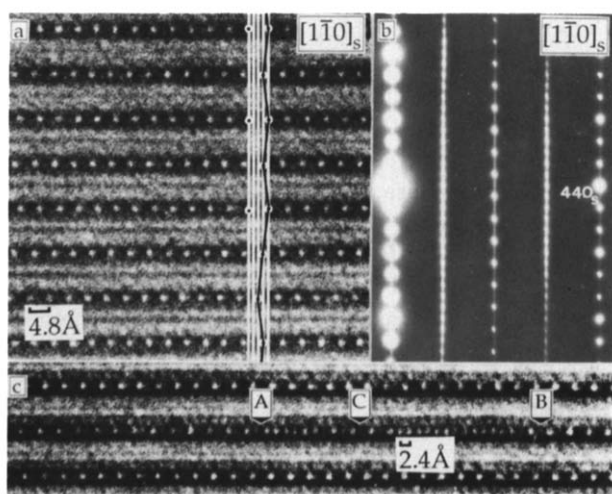


Fig. 11 High resolution image of Co-1212-phase along the  $[110]_s$  zone. Most atomic layers are imaged as lines only, due to the small intercolumn separation. In the cobalt layers the bright dots reveal the superstructure (spacing: 0.48 nm). In fig. 11a the regular stacking can be observed in the upper five dot rows; in the next row a defect appears. In fig. 11b the corresponding diffraction pattern is shown. In certain cobalt layers (fig. 11c : A to B) also the 0.24 nm spacing between bright dots is revealed indicating the presence of an intralayer line defect. Note that the widely spaced dot arrays in A (or B) and in C are out of phase. The  $[001]_s$  direction points upward.

such as  $[210]_0$  or  $[110]_s$  where  $s$  denotes the superstructure with double  $a$ -axis. Such an image (fig.11) shows bright dot rows with a spacing of 0.48 nm, which must be attributed to a superstructure (the normal spacing is only half of that, i.e. 0.24 nm). In the largest part of the area the bright dot sequences in different layers along the  $c$ -direction are shifted over one quarter of the interspot distance alternately to the left and to the right. We can show that this zig-zag arrangement is related to the staggered arrangement of the chains in successive layers.

Some of the stacking defects mentioned above are also observed here.

### Acknowledgements

The Authors are indebted to T. G. N. Babu, D. Broddin, M. Buchgeister, R. Deltour, C. Greaves, P. Herzog, S. M. Hosseini, J. Reyes-Gasga, A. Rosová, D. Wagener, A. J. Wright and H. Zou for the use of information from common papers. The work has been performed in the framework

of an IUAP-48 contract and with financial help of the National Impulse Programme on High  $T_c$  Superconductivity (SU/03/17).

### References

- 1 J.D. Jorgensen, B. W. Veal, A. P. Paulikas I. J. Nowicki, G. W. Crabtree, H. Claus and W. K. Kwok, *Phys. Rev.* B41 (1990) 1863.
- 2 B. Batlogg et al. *Novel Superconductivity* (Plenum, New York, 1987) 653.
- 3 L. A. Tietz, C. B. Carter, D. K. Lathrop, S. E. Russek, R. A. Buhrman and J. R. Michael, *J. Mater. Res.* 4 (1989) 1072.
- 4 Ø. Fischer, J.-M. Triscone, L. Antognazza, O. Brunner, A. D. Kent, L. Mieville, M. G. Karkut, *J. Less Common Metals* 164-165 (1990) 257.
- 5 Y. Tokura, *Physica C* 185-189 (1991) 174.
- 6 C. Greaves and P.R. Slater, *Physica C* 161 (1989) 245.
- 7 G. Xian et al. *Nature* 332 (1988), 238.
- 8 Y. Tokura, J.B. Torrance, T.C. Huang and A.I. Nazzari, *Phys. Rev.* B38 (1988), 7156.
- 9 T. Krekels, G. Van Tendeloo, S. Amelinckx, D. Wagener, M. Buchgeister, S. M. Hosseini and P. Herzog *Physica C* 196 (1992), 363.
- 10 T. Krekels, G. Van Tendeloo, D. Broddin, S. Amelinckx, L. Tanner, M. Mehdod, E. Vanlathem and R. Deltour, *Physica C* 173 (1991), 361.
- 11 A. Rosova, T. Krekels, G. Van Tendeloo, B. Darriet and M. Chamon, submitted to *Ferroelectrics*.
- 12 G. Roth, P. Adelman, G. Heger, R. Knitter, Th. Wolf, *J. de Physique I* 1 (1991), 721.
- 13 J.T. Vaughey, J.P. Thiel, E.F. Hasty, D.A. Groenke, C.L. Stern, K.L. Poeppelmeier, B. Dabovski, P. Radaelli, A.W. Mitchell and D.G. Hinks, *Chem. Mater.* 3 (1991), 935.
- 14 T. Krekels, T. S. Shi, J. Reyes-Gasga, G. Van Tendeloo, J. Van Landuyt and S. Amelinckx, *Physica C* 167 (1990) 677.
- 15 R. Beyers, B. T. Ahn, G. Gorman, V. Y. Lee, S. S. P. Parkin, M. L. Ramirez, K. P. Roche, J. E. Vazquez, T. M. Gür and R. A. Huggings, *Nature* 340 (1989) 619-621.
- 16 J. Reyes-Gasga, T. Krekels, G. Van Tendeloo, J. Van Landuyt, S. Amelinckx, W. H. M. Bruggink, H. Verweij, *Physica C* 159 (1989) 831.
- 17 C. N. R. Rao, R. Nagarajan, A. K. Ganguli, G. N. Subbana and S. V. Bhat, *Phys. Rev. B* 42 (1990) 6765-6768.
- 18 M. Buchgeister, W. Hiller, S. M. Hosseini, K. Kopitzki and D. Wagener, *Proceedings of the*



- of Superconductors, April 29 - May 4 1990, Rio de Janeiro, Brazil, ed. R. Nicolisky, (World Scientific Publishing, Singapore, 1990) 511-517.
- 19 D. Wagener, M. Buchgeister, P. Herzog, S. M. Hosseini, P. Seidel, G. Mertler and K. Kopitzki, preprint.
- 20 J. M. Tarascon, P. Barboux, P. F. Miceli, L. H. Greene, G. W. Hull, M. Eibschutz, S. A. Sunshine, *Phys. Rev. B* **37** (1988) 7458.
- 21 Y. Xu, M. Suenaga, J. Taftø, R. L. Sabatini, A. R. Moodenbaugh, P. Zolliker, *Phys. Rev. B* **39** (1989) 6667.
- 22 B. D. Dunlap, J. D. Jorgensen, C. Segre, A. E. Dwight, J. L. Matykiewicz, H. Lee, W. Peng and C. W. Kimball, *Phys. C* **158** (1989) 397.
- 23 T. Krekels, O. Milat, G. Van Tendeloo, S. Amelinckx, T.G.N. Babu, A. J. Wright and C. Greaves, submitted to *J. Sol. State Chem.*
- 24 O. Milat, T. Krekels, G. Van Tendeloo and S. Amelinckx, submitted to *J. Physique*.
- 25 A. Tokiwa, T. Oku, M. Nagoshi and Y. Syono, *Physica C* **181** (1991) 311.
- 26 T. Wada, A. Nara, A. Ichinose, H. Yamauchi and S. Tanaka, *Physica C* **192** (1992) 181.
- 27 R.J. Cava, R. B. Van Dover, B. Batlogg, J.J. Krajewski, L. F. Schneemeyer, T. Siegrist, B. Hessen, S. H. Chen, W. F. Peck jr. and L. W. Rupp jr., *Physica C* **185-189** (1991) 180.